Measurements of the parallel and transverse Spitzer resistivities during collisional magnetic reconnection[a)]

A. Kuritsyn,[b)] M. Yamada, S. Gerhardt, H. Ji, R. Kulsrud, and Y. Ren
Center for Magnetic Self-Organization in Laboratory and Astrophysical Plasmas, Princeton Plasma Physics Laboratory, Princeton, New Jersey 08543

(Received 31 October 2005; accepted 29 December 2005; published online 10 May 2006)

Plasma resistivity has been studied experimentally in a reconnecting current sheet. Resistivities during collisional reconnection, when the electron mean free path is much shorter than the current sheet thickness, in the presence and absence of the guide field are found to be in a good agreement with the parallel and transverse Spitzer values, respectively. © *2006 American Institute of Physics*. [DOI: 10.1063/1.2179416]

I. INTRODUCTION

Electrical resistivity is one of the most important quantities in plasma physics, as it is related to the electron transport and magnetic energy dissipation rate. The classical plasma resistivity[1] is the rate of momentum transfer between electrons and ions through Coulomb collisions in response to an applied electric field. The electric field produces force on charged particles in a plasma, accelerating electrons in one direction and ions in the opposite direction. Collisions between electrons and ions impede this relative motion and equilibrium is reached when the driving force on an electron produced by the electric field is balanced by a resistive drag force. In many realistic situations resistivity is often enhanced due to neoclassical effects, such as geometry and trapped particles,[2,3] or dominated by turbulent transport. Nevertheless, the classical value presents an irreducible minimum value for this transport coefficient.

Spitzer[1] showed that to obtain an accurate theoretical value of classical resistivity two effects have to be taken into account. First of all, the electron distribution function gets distorted from a simple shifted Maxwellian because electrons with larger velocities experience fewer collisions with ions, as the Coulomb collision frequency is inversely proportional to the third power of velocity ($\nu_{ei} \sim 1/v^3$), and are thus accelerated more. Secondly, electron-electron collisions provide friction drag on the high velocity tail of the distribution function, leading to its Maxwellization. After incorporating these effects, the resistivity $\eta_\parallel$ along the magnetic field or in the unmagnetized plasma can be represented in the form:[2]

$$\eta_\parallel^{\text{Spitzer}} = \frac{\sqrt{2m_e}Z_{\text{eff}}e^2 \ln \Lambda}{12\pi^{3/2}\epsilon_0^2 T_e^{3/2}} \times F(Z_{\text{eff}}), \tag{1}$$

where T_e is the electron temperature, Z_{eff} is the effective ionic charge, $\ln \Lambda = \ln(T_e^{3/2}/\sqrt{\pi Z e^3 n^{1/2}})$ is the Coulomb logarithm, and $F(Z_{\text{eff}})$ is approximated by:

$$F(Z) \simeq \frac{1 + 1.198Z + 0.222Z^2}{1 + 2.966Z + 0.753Z^2}. \tag{2}$$

Thus, in the important case of Z_{eff} equal to 1,

$$\eta_\parallel^{\text{Spitzer}}[\text{Ohm} \times \text{m}] = 0.53 \times 10^{-4} \frac{\ln \Lambda}{T_e^{3/2}[\text{eV}]}. \tag{3}$$

Since binary collisions leading to a large angle scattering are neglected in the Spitzer calculation, the final result has the uncertainty of $1/\ln \Lambda$.[4]

The main assumptions of the unmagnetized Spitzer calculation are the following: (1) steady-state, (2) energy gained by an electron due to acceleration in the electric field between collisions is negligible compared to the electron thermal energy ($eE\lambda_{\text{mfp}} \ll kT$), which means that the electron distribution function does not strongly deviate from Maxwellian, and (3) plasma is completely ionized, so collisions with neutrals are negligible.

Spitzer also demonstrated that for the case when a strong uniform magnetic field ($\rho_e \ll \lambda_{\text{mfp}}$) is applied perpendicular to the direction of electric field and plasma current, the cross-field or transverse resistivity is approximately twice as large as the parallel resistivity for $Z_{\text{eff}}=1$:

$$\eta_\perp^{\text{Spitzer}} = 1.96 \times \eta_\parallel^{\text{Spitzer}}. \tag{4}$$

For larger Z_{eff} the ratio $\eta_\perp/\eta_\parallel$ increases (see Table 1 of Ref. 5). This difference between parallel and transverse resistivities comes from the fact that the electron distribution functions are quite different for the currents flowing along and across the magnetic field. In the parallel case (or unmagnetized plasma), the current is carried by fast suprathermal electrons at the tail of the Maxwellian distribution function experiencing less frequent collisions. In the cross-field current case, the distribution of current over the electrons of different velocities is altered and more electrons contribute to the total current. This leads to the resistivity increase.

This article presents a study of plasma resistivity done in the well controlled laboratory environment of the Magnetic Reconnection eXperiment (MRX).[6] In our previous paper[7] we reported measurements of the transverse Spitzer resistivity during collisional magnetic reconnection without a guide

[a)]Paper BI2 5, Bull. Am. Phys. Soc. **50**, 23 (2005).
[b)]Invited speaker. Present address: Department of Physics, University of Wisconsin-Madison, Madison, Wisconsin 53706. Electronic mail: kuritsyn@wisc.edu

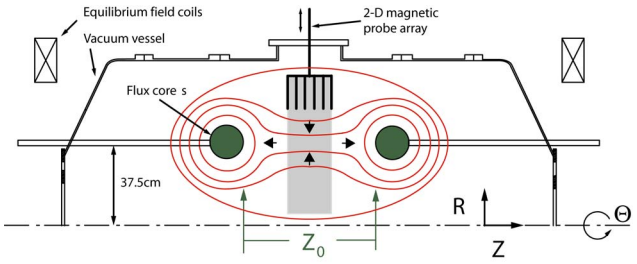

FIG. 1. (Color online) Schematic of the MRX apparatus cross section. Flux contours indicate the current sheet between the flux-cores with the current flowing in the Θ direction.

field. The versatility of the MRX facility also allows to check Spitzer theory by performing measurements of parallel resistivity during collisional reconnection in the presence of a guide field and to compare it to the case without a guide field. These measurements will be the main focus of the article.

II. MRX APPARATUS AND DIAGNOSTICS

A cross-sectional view of the MRX apparatus is shown in Fig. 1. Two flux-cores are used to create plasma and to drive reconnection. Each flux-core has two sets of coil windings, which produce toroidal (TF) and poloidal (PF) magnetic fields. The spacing Z_0 between the flux-cores along the symmetry axis can be varied. In the course of the experiment an "X-point" like magnetic configuration is first established by pulsing currents in the PF coils. Currents in the TF coils are then pulsed, which create inductive electric fields around the flux-cores and cause gas break down. Depending on the mutual orientation of the TF currents in the flux-cores, discharges without a guide (B_Θ component) magnetic field (null-helicity) and with the guide field (co-helicity) can be studied. When PF field currents are ramped down, poloidal flux is pulled back towards the flux-cores and an inductive electric field E_Θ is induced in the toroidal direction. As a result, a toroidally symmetrical current sheet is formed with current flowing along the Θ direction.

Plasma current is driven differently with or without a guide field. In the co-helicity case the current is mainly caused by direct acceleration of electrons by the electric field E_Θ. In the null-helicity case, however, the current is not due to direct acceleration of electrons by the electric field, but is diamagnetic in origin. Oppositely directed magnetic field lines frozen into the plasma are convected towards each other by fluid flow caused by $E_\Theta \times B_Z$ drift. As a result, in the null-helicity regime, strong plasma pressure and magnetic field gradients are created in the diffusion region generating diamagnetic current. In the co-helicity regime the guide field peaks in the center of the current sheet as a result of paramagnetic effect (see Fig. 9 in Ref. 6), which leads to the development of a broader current sheet than in the null-helicity case. The spatial gradients of plasma pressure and magnetic field pressure are thus reduced resulting in the reduction of the diamagnetic current.

The reconnection process in MRX is well diagnosed. Because of relatively low plasma temperature and short discharge time ($\leqslant 100$ μs) internal probes are used routinely. Extensive sets of magnetic probes (pick-up coils) allow accurate mapping of the magnetic field and calculation of the poloidal flux assuming toroidal symmetry: $\psi(R,Z,t) = \int_0^R 2\pi R' B_z(R',Z,t)dR'$. Examples of the vector plots measured by the 90-channel magnetic probe array at flux-core separations $Z_0=35$ cm and $Z_0=60$ cm are displayed in Fig. 2. The electric field is determined from Faraday's law: $E = -(d\psi/dt)/2\pi R$. The magnetic field in the field reversal region is measured precisely by a linear array of pick-up coils (1D probe) spaced 0.5 cm apart. An earlier study[8] showed that radial profile of the reconnecting field B_Z is well described by the Harris-type profile.[9] The current density profile is then deduced as the derivative of the hyperbolic tangent fit to the measured magnetic field profile: $j_\theta \approx -(\partial B_z/\partial R)/\mu_0$. The plasma density and electron temperature are simultaneously measured by a triple Langmuir probe. Values of the electron temperature measured by the triple probe have been verified by scanning bias voltage of a double Langmuir probe and spectroscopically by measuring the intensity ratio of two He I lines and implementing a coronal model. The systematic error of the electron temperature measurements was found not to exceed 20%.[7] The typical MRX plasma parameters are as follows: density $n=0.1-2 \times 10^{20}$ m^{-3}, electron temperature $T_e=3-15$ eV, magnetic field $B<0.5$ kG. In the experiments described below deuterium was used as the fill gas unless otherwise noted.

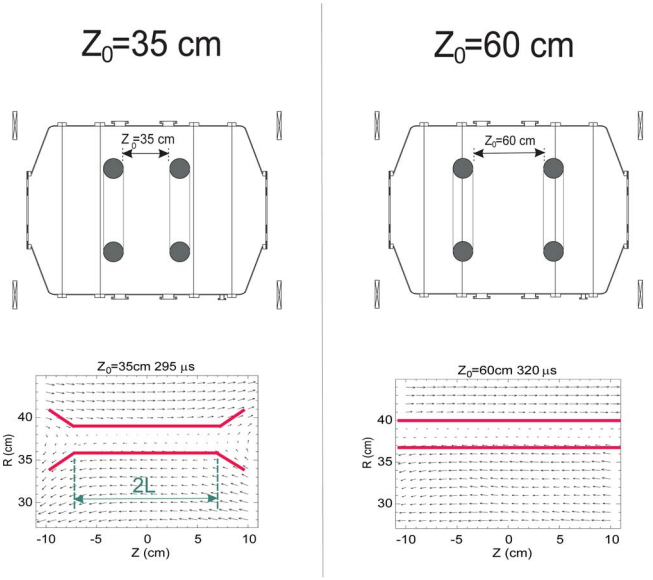

FIG. 2. (Color online) Illustration of the experimental setup and magnetic field vector plots measured by the 90-channel magnetic probe array at flux-core separation of (left) $Z_0=35$ cm and (right) $Z_0=60$ cm in the high collisionality null-helicity regime. Solid lines schematically show the current sheet.

III. APPLICATION OF THE SPITZER THEORY TO MRX

To verify that Spitzer's formulation in fact applies to the MRX current sheets let us examine assumptions of his theory in detail. Depending on the collisionality parameter, defined as the ratio of the current sheet thickness to the electron mean free path, different experimental regimes can be

achieved in MRX. In these regimes resistivity can be either classical or "anomalous." In the collisional regime, where the electron mean free pass is shorter than the current sheet thickness, most of the assumptions of the Spitzer theory are satisfied. (1) The electron collision time (~20 ns) is much shorter than the reconnection time scale (~20 μs), so electron distribution function reaches steady state. (2) The Dreicer field is much smaller than the reconnecting electric field E_0 in the collisional regime (but can be comparable to the reconnecting field at low collisionality). (3) It has been shown in Ref. 7 through an analysis of the Fokker-Plank equation that the applicability of the Spitzer theory can be extended into the regime with nonuniform magnetic field. Therefore, the Spitzer theory is expected to be valid in the nonuniform field reversal region of MRX in the null-helicity regime. The magnetized theory, however, breaks down close to the magnetic null point, as electrons do not undergo gyromotion but instead have meandering orbits ("figure eight" and betatron). The spatial extent of this region can be estimated from the condition that the electron gyro-radius is equal to the distance to the null point $\rho_e(d_{er})=d_{er}$.[10] Assume that the magnetic field in the vicinity of the field reversal region is, to the first order, changing linearly as $B_Z(r)=B_Z(\delta)\cdot r/\delta$, where δ is the current sheet half-thickness. Then $d_{er}=\sqrt{\rho_e(\delta)\cdot\delta}=1.7$ mm for typical experimental parameters of $\rho_e=0.2$ mm and $\delta=1.5$ cm. This scale is small compared to the spatial resolution of the magnetic probes, so one would expect no major effect on the results of the measurements.

The effect of the reconnecting magnetic field B_Z on the parallel resistivity in the co-helicity regime can be estimated in a following way. Because of the reconnecting magnetic field present near the current sheet center, electrons do not exactly move in the toroidal direction, but have a spiral trajectory. The magnetic field has a screw factor $q=rB_\Theta/RB_Z \simeq 0.13$ (assuming $B_Z\approx B_Z^0\cdot r/\delta$ near the center of the current sheet, $R=37.5$ cm, $\delta=5$ cm, $B_\Theta/B_Z^0\approx 1$). The length of the field line is then $ds=Rd\Theta(1+(r/Rq)^2)^{1/2}=Rd\Theta(1+(r/\delta)^2)^{1/2}$. Hence, as long as $r\ll\delta$, electrons primarily move in the Θ direction and the notion of the parallel resistivity is valid. For example, for $r\simeq 2$ cm the parallel plasma resistivity is still close to the Spitzer value: $\eta^{\mathrm{Co}}/\eta_\parallel^{\mathrm{Spitzer}} \simeq \sqrt{1+(0.4)^2}\simeq 1.1$.

IV. EXPERIMENTAL RESULTS

In MRX, reconnection proceeds in a quasi steady-state manner for about 10 Alfven times (20–30 μs), during which the current sheet is spatially stationary. Since the electric field, current density and inflow speed can be simultaneously measured, one can quantitatively study the toroidal component of Ohm's law during this time interval:

$$E_\Theta - V_R \times B_Z = \eta j_\Theta. \tag{5}$$

In the center of the current sheet, where $B_Z\simeq 0$, the second term on the left-hand side vanishes and the plasma resistivity η can be determined as the ratio of the toroidal electric field E_Θ to the current density j_Θ measured at the current sheet center. To study the dependence of resistivity on collisionality, the plasma collisionality was varied by changing the neutral gas fill pressure at fixed firing voltage. Results of the pressure scan in the co-helicity regime at a flux-core separation of $Z_0=50$ cm are displayed in Fig. 3.

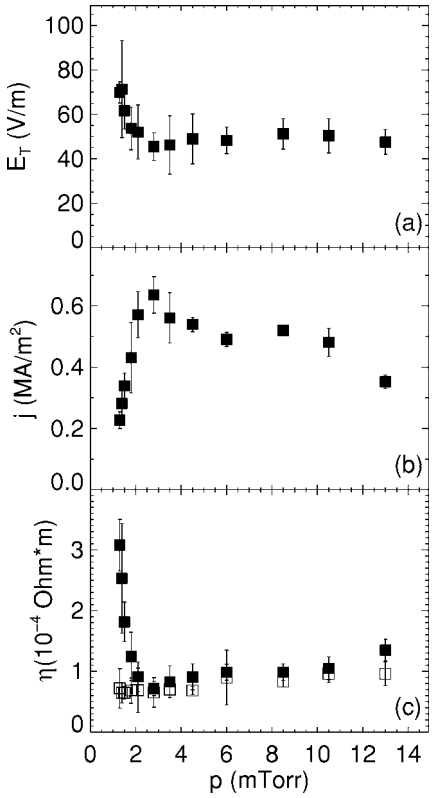

FIG. 3. (a) Toroidal electric field, (b) current density, and (c) resistivity versus neutral fill pressure for co-helicity discharges in deuterium at $Z_0=50$ cm flux-core spacing. Open symbols in (c) correspond to $\eta_\parallel^{\mathrm{Spitzer}}$.

Figure 4 presents the dependence of the measured plasma resistivity normalized to the Spitzer value on the inverse collisionality at different flux-core separations in the (a) null-helicity and (b) co-helicity regimes. The inverse collisionality is defined as the ratio of the electron mean free path to the current sheet thickness. The effective ionic charge Z_{eff} is set to 1 in the calculation of Spitzer values in accordance to the earlier study performed in Ref. 7. At high collisionality, the measured resistivity is very close to the perpendicular Spitzer value in the null-helicity regime and parallel Spitzer value in the co-helicity regime. When the collisionality is reduced, the resistivity is enhanced. The normalized resistivities have similar dependence on the inverse collisionality parameter at different flux-core separations. However, the current sheet thickness δ was becoming larger as flux-core spacing was increased and somewhat longer mean free pass was required to achieve similar resistivity enhancement at larger flux-core separations. The cause of the resistivity enhancement at low collisionality is the main focus of the MRX research with two major possibilities being addressed: (1) resistivity can be enhanced due to turbulence associated with electromagnetic fluctuations in the lower-hybrid frequency range observed in the MRX current sheet[11,12] and (2) two-fluid effects can be important in balancing the reconnecting electric field.[13] Discussion of these

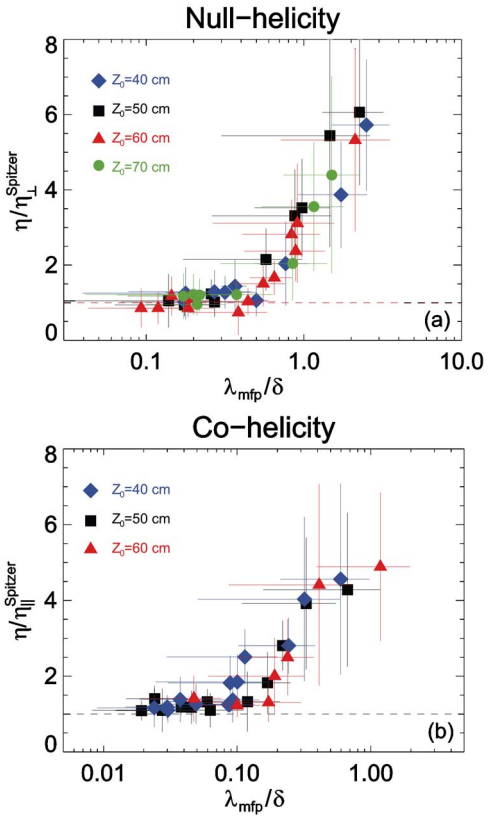

FIG. 4. (Color online) (a) Effective plasma resistivity normalized to the transverse Spitzer resistivity ($\eta/\eta_\perp^{\text{Spitzer}}$) as a function of inverse collisionality $\lambda_{\text{mfp}}/\delta$ for different flux core separations Z_0 in null-helicity deuterium discharges. (b) Effective plasma resistivity normalized to the parallel Spitzer resistivity ($\eta/\eta_\parallel^{\text{Spitzer}}$) versus inverse collisionality $\lambda_{\text{mfp}}/\delta$ at different flux-core separations Z_0 in co-helicity deuterium discharges.

theories will be a subject of a separate publication.

A comparison of the resistivity in null-helicity and co-helicity discharges in the high-collisionality regime is presented in Fig. 5, where $\eta^{\text{Null}}/\eta_\parallel^{\text{Spitzer}}$ and $\eta^{\text{Co}}/\eta_\parallel^{\text{Spitzer}}$ are plotted at different flux-core spacings. The values of resistivity shown on the graph are obtained through averaging the measured resistivity normalized to the parallel Spitzer resistivity over points at short mean free path (high collisionality). The error bars represent the 30% systematic uncertainty due to

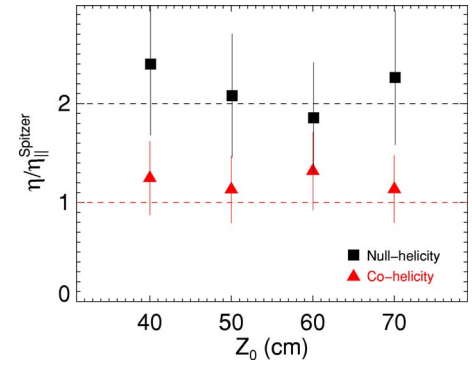

FIG. 5. (Color online) Comparison of resistivities in the collisional regime in null-helicity and co-helicity deuterium discharges normalized to the $\eta_\parallel^{\text{Spitzer}}$. Error bars represent 30% uncertainty due to electron temperature measurement errors.

electron temperature measurements, which is bigger than the error associated with shot-to-shot variations. The absolute values of the resistivities are similar in the two cases. However one is equal to $\eta_\perp^{\text{Spitzer}}$ and the other to $\eta_\parallel^{\text{Spitzer}}$, because the electron temperature in the co-helicity regime is smaller by about 40%. This temperature difference is consistent with the fact that there is an additional magnetic field pressure in the center of the current sheet in the co-helicity case. This pressure acts against current sheet compression and leads to the development of a broader current sheet profile with current density lower than in the null-helicity case. This results in reduced Ohmic heating in the center of the current sheet and consequently a lower electron temperature if thermal losses are similar.

The effect of electron-neutral collisions on resistivity is neglected in the Spitzer calculation. Since the peak plasma density is $n_e=1-10\times10^{19}$ m^{-3} for the neutral gas fill pressure of 2–15 mT, the ionization fraction during MRX discharge is smaller than 40%. Therefore, it is essential to evaluate how electron-neutral collisions contribute to the resistivity. The typical integrated momentum cross section for *e-D* elastic collisions at 5 eV electron temperature is $\sigma_m=1\times10^{-15}$ cm^2 and collision rate coefficient is $\langle\sigma_m V\rangle\simeq10^{-7}$ cm^3/s.[14] Nonelastic collisions are not important at these plasma parameters, since the ionization cross section is much smaller than the cross section for elastic collisions. For the fill pressure $p=6$ mT, plasma density of $n_e=8\times10^{13}$ cm^{-3}, and assuming neutrals can freely penetrate to the current sheet, $\nu_{en}=n_n\langle\sigma_m V\rangle=12$ MHz. This is much smaller than the electron-ion collision frequency $\nu_{ei}=104$ MHz ($T_e=4.5$ eV, $Z_{\text{eff}}=1$). Therefore, electron-neutral collisions do not have a strong effect on resistivity in deuterium (and hydrogen) discharges.

Electron-neutral collisions, however, can play an important role in high density helium discharges. The electron temperature is observed to be higher and the plasma density is lower in helium discharges, as compared to deuterium at the same firing voltages and fill pressures. Consequently, higher gas fill pressure is required to achieve collisional plasma in helium discharges (with $\lambda_{\text{mfp}}\ll\delta$). Also, since the electron temperature is higher in helium discharges, this reduces the electron-ion collision frequency ν_{ei}. High density and high collisionality helium discharges are usually achievable at fill pressures $p_{\text{fill}}>13$ mT. In this regime the electron-ion collision frequency $\nu_{ei}=30$ MHz ($T_e=10$ eV, $Z_{\text{eff}}\simeq1$) is comparable to the frequency of the elastic electron-neutral collisions $\nu_{en}=25$ MHz [$\langle\sigma_m V\rangle\simeq8\times10^{-8}$ cm^3/s (Ref. 15)]. Thus, the effect of electron-neutral collisions can explain why the experimentally measured resistivity is typically larger by about a factor of 2 than $\eta_\perp^{\text{Spitzer}}$ in the high-collisionality null-helicity helium discharges.

V. CONCLUSIONS

In summary, the parallel and transverse plasma resistivities during collisional ($\lambda_{\text{mfp}}\ll\delta$) magnetic reconnection in deuterium discharges in the presence and absence of the guide magnetic field are found to be in agreement with the Spitzer theory within 30% accuracy. The measured plasma

resistivity in the null-helicity case is equal to the transverse Spitzer value and in the co-helicity case to the parallel Spitzer value. Contribution of the electron-neutral collisions to the resistivity is found to be negligible in the deuterium discharges. In contrast, in helium discharges they can explain deviation of the measured resistivity from the Spitzer value.

ACKNOWLEDGMENTS

The authors would wish to thank R. Cutler and D. Cylinder for excellent technical support.

The MRX is jointly funded by DOE, NASA, and NSF.

[1] L. Spitzer, *Physics of Fully Ionized Gases* (Interscience, New York, 1962).
[2] M. Zarnstorff, K. McGuire, M. G. Bell, B. Grek, D. Johnson, D. McCune, H. Park, A. Ramsey, and G. Taylor, Phys. Fluids B **2**, 1852 (1990).
[3] J. Egedal, A. Fasoli, D. Tarkowski, and A. Scarabosio, Phys. Plasmas **8**, 1935 (2001).
[4] L. Spitzer, Phys. Rev. **89**, 977 (1953).
[5] S. I. Braginskii, *Transport Processes in a Plasma. Reviews of Plasma Physics*, edited by M. A. Leontovich (Consultants Bureau, New York, 1965), Vol. 1, pp. 205–311.
[6] M. Yamada, H. Ji, S. Hsu, T. Carter, R. Kulsrud, N. Bretz, F. Jobes, Y. Ono, and F. Perkins, Phys. Plasmas **4**, 1936 (1997). H. Ji, M. Yamada, S. Hsu, and R. Kulsrud, Phys. Rev. Lett. **80**, 3256 (1998).
[7] F. Trintchouk, M. Yamada, H. Ji, R. M. Kulsrud, and T. A. Carter, Phys. Plasmas **10**, 319 (2003).
[8] M. Yamada, H. Ji, S. Hsu, T. Carter, R. Kulsrud, and F. Trintchouk, Phys. Plasmas **7**, 1781 (2000).
[9] E. G. Harris, Nuovo Cimento **23**, 115 (1962).
[10] M. M. Kuznetsova, M. Hesse, and D. Winske, J. Geophys. Res. **105**, 7601 (2000).
[11] H. Ji, S. Terry, M. Yamada, R. Kulsrud, A. Kuritsyn, and Y. Ren, Phys. Rev. Lett. **92**, 115001 (2004).
[12] R. Kulsrud, H. Ji, W. Fox, and M. Yamada, Phys. Plasmas **12**, 082301 (2005).
[13] Y. Ren, M. Yamada, S. Gerhardt, H. Ji, R. Kulsrud, and A. Kuritsyn, Phys. Rev. Lett. **95**, 055003 (2005).
[14] J. F. Williams, J. Phys. B **8**, 1683 (1975).
[15] J. C. Nickel, K. Imre, D. F. Register, and S. Trajmar, J. Phys. B **18**, 125 (1985).